JPE 16-1-20

http://dx.doi.org/10.6113/JPE.2016.16.1.182
ISSN(Print): 1598-2092 / ISSN(Online): 2093-4718

Fault Detection of a Proposed Three-Level Inverter Based on a Weighted Kernel Principal Component Analysis

Mao Lin†, Ying-Hui Li*, Liang Qu*, Chen Wu*, and Guo-Qiang Yuan*

*School of Aeronautics and Astronautics Engineering, Air Force Engineering University, Xi'an, China

Abstract

Fault detection is the research focus and priority in this study to ensure the high reliability of a proposed three-level inverter. Kernel principal component analysis (KPCA) has been widely used for feature extraction because of its simplicity. However, highlighting useful information that may be hidden under retained KPCs remains a problem. A weighted KPCA is proposed to overcome this shortcoming. Variable contribution plots are constructed to evaluate the importance of each KPC on the basis of sensitivity analysis theory. Then, different weighting values of KPCs are set to highlight the useful information. The weighted statistics are evaluated comprehensively by using the improved feature eigenvectors. The effectiveness of the proposed method is validated. The diagnosis results of the inverter indicate that the proposed method is superior to conventional KPCA.

Key words: Fault detection, Kernel principal component analysis (KPCA), Sensitivity analysis, Three-level inverter

I. INTRODUCTION

Nowadays, the application of three-level inverters to distributed generation, energy storage systems, and uninterruptible power supply has gained considerable research attention because these inverters have lower harmonics content and less electromagnetic interference than two-level inverters at the same switching frequency [1]. However, the three-level inverter still has some shortcomings; three-level inverters have more components compared with two-level inverters because the latter comprise many semiconductor devices. The large number of devices translates into reduced reliability of the system because any device failure may cause the abnormal operation of the inverter and economic losses [2], [3]. Therefore, the inverter must achieve high reliability.

Switching device faults are always the main concern for a multilevel inverter; these faults can be classified into a short-circuit switch fault and an open switch fault [4]. Short-circuit faults are difficult to cope with because fault initiation and failure are small, and the protection strategies are mostly hardware based [5]; therefore, the present research focuses on open switch detection. The open-switch fault does not require the system to be shut down in an instant. However, it can induce noise and vibrations in the system because of non-symmetrical currents [6]. Therefore, if an open-switch fault is addressed immediately, then it can cause secondary problems in other parts. Thus, monitoring switching device faults and identifying the device in which the fault has occurred are important to reduce the cost of repairs and to improve the stability and reliability of the device.

Fault detection methods are the bases of implementing a fault-tolerant operation. A number of open-switch fault detection methods exist and can be divided into two categories: the first strategy is a model-based approach, such as Park's vector method in [7] open-circuit fault detection. Detect transistor localization is accomplished by calculating the position of the current trajectory midpoint; the defect transistor is identified by the phase angle, but it still relies heavily on the experience of an engineer and may fail to find the hidden faults of the circuit. Converter behavior method [8] is a method based on measurement of DC bus current in each leg, AC currents, and voltages. However, defining a complete switching behavior of the power converter needs extensive computation and additional sensors. The second strategy is the data processing approach [9], which is a fuzzy logic-based technique that detects and identifies faulty switches in a

Manuscript received Jun. 2, 2015; accepted Sep. 11, 2015
Recommended for publication by Associate Editor Kyo-Beum Lee.
†Corresponding Author: 496180444@qq.com
Tel: 0913-84787606, Air Force Engineering University
*School of Aeronautics and Astronautics Engineering, Air Force Engineering University, China

voltage-fed pulse width modulation inverter for an induction motor drive by using current patterns. However, this method requires a relatively long diagnosis time. In [10], a fault diagnosis scheme was proposed to detect and identify the location of a fault in a multilevel inverter by using a neural network algorithm. However, this technique requires extensive computation.

Kernel principal component analysis (KPCA) is a data processing method. The KPCA maps the input vector until a high-dimensional feature space achieves non-linear mapping through a kernel function and the PCs in the feature space are computed. Then, the principal element of the mapping data of high-dimensional space is analyzed. The KPCA does not involve nonlinear optimization unlike other nonlinear strategies [11], [12]. Therefore, the KPCA is suitable for solving nonlinear problems. Nevertheless, for a definite fault, the KPCA usually causes one or several specific variable variations; hence, other KPCs that are employed may not have the same variation degree [13]. In other words, for different fault cases, KPCs may have different variations. Employing KPCs with larger variation, which contain more fault information, can find faults more quickly compared with KPCs with less variation or without variation and contain less fault information. Thus, the kind of KPCs that should be employed may not always be the same because some KPCs would reflect more information on certain faults, whereas others would reflect less. Moreover, KPS with less or even without variation may not detect faults at all and thus give poor results. Therefore, the improved weighting strategy should be introduced to highlight the degree of importance of each employed KPC with regard to fault information.

This paper proposes a detection method of an open switch fault for a new three-level inverter. Sensitivity analysis theory is introduced to solve the problem on submerged useful information by choosing the weight matrix dependent on the variable contribution to the fault detection and improve the performance in detecting insulated-gate bipolar transistor (IGBT) faults. Then, the proposed detection method is tested in the proposed topology fault process, with the conventional KPCA and improved KPCA presented.

II. PRELIMINARIES

A. Operation of the New Inverter

The proposed topology of the inverter is shown in Fig. 1. The topology is composed of two symmetrical two-level inverters in series by transformers T_1 and T_2. Each transformer has six active switches, of which switches S_{n1}–S_{n4} are added to achieve voltage balance on the dc-link capacitors for any operating condition. In this research, the active switches are IGBTs. The inverter output voltages have higher harmonics because of the switching of the power semiconductors. Thus, the inverter is connected to the load

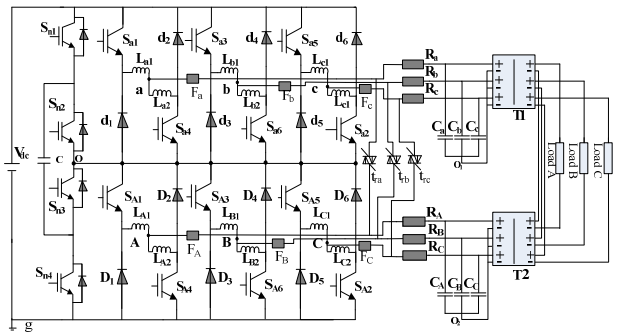

Fig. 1. New inverter topology.

TABLE I
SWITCH STATES OF ONE PHASE

$(S_{a1}, S_{a4}, S_{A1}, S_{A4})$	(U_{ag}, U_{Ag})
(1,0,1,0)	$(V_{dc},V_{dc}/2)$
(0,1,0,1)	$(V_{dc}/2,0)$
(0,1,1,0)	$(V_{dc}/2,V_{dc}/2)$
(1,0,0,1)	$(V_{dc},0)$

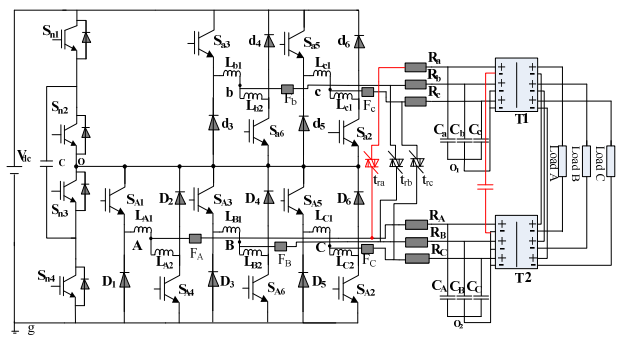

Fig. 2. Fault-tolerant method of single IGBT fault.

through an *LC* filter to provide a high-quality sinusoidal voltage.

The relation of switch states for phase A of inverter is shown in Table I; similar to the rest of the two phases, U_{ag} is the voltage between a and g, and U_{Ag} is the voltage between A and *g*.

Several different faults can occur within a three-level voltage source inverter. The probability of failure in semiconductors is high and should be taken into consideration. Several factors can cause failures, such as transistor short circuit and transistor open circuit. The original NPC topology was changed by applying a symmetrical structure of two-level inverters. For example, suppose that an open circuit failure of the S_{a1} power switch occurs (phase A) while the inverter is supplying a three-phase nonlinear load. The first step is to add fast fuse F_a to cut off the failure circuit by t_{ra} connecting the failure leg to the symmetry half-bridge to achieve continuous work by the traditional two-level inverters (which is depicted in red color in Fig. 2). In addition, connecting the negative of the faulty output to the output of the symmetry leg is necessary. The

TABLE II
NEW INVERTER FAULT TOLERANT METHOD

Fault mode	Fault tolerant schemes
Single bridge fault	Connect to summary bridge arm
Two bridges fault	Connect to summary bridge arms
Three bridges fault	Connect to summary bridge arms

symmetry half-bridge takes care of the replacement of the damaged phase. The proposed topology has the additional redundancy to solve the semiconductor's fault problems.

The other bridge arms fault tolerant strategy can be obtained from Table II. Therefore, the system can provide practically full power in the event of a fault.

B. Kernel Principal Component

In KPCA, the original data are nonlinearly mapped into high-dimensional feature space H, and PCA is performed to acquire the intrinsic information between the variables. Let the normalized training set be $x_i \in \mathrm{R}^m, i=1,\ldots,n$. The high dimensional space is constructed by nonlinear mapping: $\Phi: x_i \rightarrow H$, where $\Phi(\bullet)$ is mean centered and variance scaled. We obtained the following covariance matrix in the feature space H:

$$C^H = \frac{1}{n}\sum_{i=1}^{n}\Phi(x_i)\Phi(x_i)^{\mathrm{T}} . \quad (1)$$

The kernel principal component can be obtained by solving the following eigenvalue problem:

$$\lambda v = C^H v = \frac{1}{n}\sum_{i=1}^{n}\Phi(x_i)\Phi(x_i)^{\mathrm{T}} v = \frac{1}{n}\sum_{i=1}^{n}\langle\Phi(x_i), v\rangle\Phi(x_i) \quad (2)$$

where eigenvalue $\lambda>0$ and eigenvector $v \in H$. Note that (x,y) denotes the dot product of two elements, which is defined by Mercer kernel as

$$k_h(x,y) = \langle\Phi(x), \Phi(y)\rangle . \quad (3)$$

All solutions v with $\lambda \neq 0$ must lie in the range of $\Phi(x_1),\cdots\Phi(x_n)$, $v = \sum_{i=1}^{n}\alpha_i\Phi(x_i)$. Hence, $\lambda v = C^H v$ is equivalent to

$$n\lambda\alpha = K\alpha \quad (4)$$

where $\alpha=[\alpha_1,\alpha_2,\ldots,\alpha_n]^{\mathrm{T}}$, and $K \in \mathrm{R}^{n\times n}$ is the Gram matrix, which is defined by

$$K_{ij} = \langle\Phi(x_i), \Phi(x_j)\rangle = k_h(x_i, x_j) . \quad (5)$$

Let principal components t of test vector x be a test point with image $\Phi(x)$ in H, as follows:

$$t_l = \sum_{i=1}^{n}\bar{a}_i^l\langle\bar{\Phi}(x_i), \bar{\Phi}(x_k)\rangle = \sum_{i=1}^{n}\bar{a}_i^l\bar{k}_h(x_i, x_k) = \bar{K}_h\bar{a}^l \quad (6)$$

where $l=1,2,\ldots,r$, r is selected as the principal component number (the significance level is set to α=99% for all methods), and $\bar{\alpha}^l$ is the center eigenvector. The centered kernel matrix is denoted by $\bar{K}_h$ as

$$\bar{K}_h = K_k - I_0K - K_kE_0 + I_0KE_0 \quad (7)$$

where $I_0 \in \mathrm{R}^{n\times n}$, each element of I_0 is $1/n$, and E_0 is the identity matrix.

In the KPCA-based fault detection, statistics and their control limits should be established to determine whether a process is in control or not. Common statistics include Hotelling's T^2 statistic, which reflects the variations with KPCA model, and the squared prediction error (SPE) statistic (also known as Q statistic), which indicates the degree of deviation of each sample from the model. The two statistics and corresponding control limits are defined as follows:

$$\begin{cases} T^2 = [t_1, t_2, \ldots, t_r]\Lambda^{-1}[t_1, t_2, \ldots, t_r]^{\mathrm{T}} \\ Q = \left\|\Phi(x_k) - \Phi_r(x_k)\right\|^2 = \sum_{i=1}^{p} t_i^2 - \sum_{i=1}^{r} t_i^2 \end{cases} \quad (8)$$

where t_i is obtained from Equ. (6), and Λ^{-1} is the diagonal matrix of the inverse of the eigenvalue associated with the retained PCs. The confidence limit for T^2 is obtained using F distribution, and the confidence limit for the SPE can be computed from its approximate distribution as

$$\begin{cases} T_\alpha^2 = \dfrac{r(n^2-1)}{n(n-r)}F_\alpha(r, n-r) \\ Q_\alpha = g\chi^2(h) \end{cases} \quad (9)$$

where $F_\alpha(r, n-r)$ is an F distribution with degree of freedom r, and $(n-r)$ and with level of significance α. n is the number of samples in the model, and r is the number of PCs. $g=b/2a$ and $h=2a^2/b$, where a and b are the estimated mean and variance of the SPE, respectively. If the SPE statistic shows an unexpectedly large value, then the data points go into the residual subspace. When T^2 statistic shows unexpected values, a deviation from normal values in PC subspace exists.

III. SENSITIVITY ANALYSIS FOR KPCA FAULT DETECTION

A. Weighting Matrix based on Sensitivity Analysis

For the traditional KPCA-based fault detection methods, the T^2 and *SPE* statistic are constructed to detect the variations of the first several kernel principal components because the distributions of all variables are assumed to have the same covariance matrix [14]. However, for a certain KPC, fault information that is quite different from the others and the KPCs are not of equal importance. If the information is relatively limited, then the useful KPCs could be suppressed by the useless ones, thus submerging the useful information [15], [16]. Therefore, adapting covariance matrix to different classes of information is necessary. In this research, an improved KPCA fault detection method based on sensitivity analysis is proposed for the IGBT faults.

Next, the weighted KPCA is present. In weighting matrix *W*, important kernel principal components should be heavily weighted, and large corresponding weighting values should be assigned. In this section, we build a contribution plot method, based on a sensitivity analysis, which calculates the rates of change in the system output variables that result from small perturbations in the problematic parameters, defining variable contributions to the T^2 and *SPE* statistics as a vector form

$$\begin{cases} C_{T^2}(x_{kj}) = x_{kj}\dfrac{\partial T^2}{\partial x_{kj}} \\ C_Q(x_{kj}) = x_{kj}\dfrac{\partial Q}{\partial x_{kj}} \end{cases}. \tag{10}$$

We can rewrite Equ. (10) as

$$C_{T^2}(x_{kj}) = x_{kj}\frac{\partial T^2}{\partial x_{kj}} = x_{kj}\frac{\partial([t_1,t_2,...,t_r]\Lambda^{-1}[t_1,t_2,...,t_r]^{\mathrm{T}})}{\partial x_{kj}} = x_{kj}\frac{\partial(\sum_{i=1}^{r}\frac{t_i^2}{\lambda_i})}{\partial x_{kj}} = 2x_{kj}\sum_{i=1}^{r}\frac{t_i}{\lambda_i}\frac{\partial t_i}{\partial x_{kj}} \tag{11}$$

$$C_Q(x_{kj}) = x_{kj}\frac{\partial Q}{\partial x_{kj}} = x_{kj}\frac{\partial(\sum_{i=1}^{p}t_i^2 - \sum_{i=1}^{r}t_i^2)}{\partial x_{kj}} = x_{kj}\frac{\partial(\sum_{i=r+1}^{p}t_i^2)}{\partial x_{kj}} = 2x_{kj}\sum_{i=r+1}^{p}t_i\frac{\partial t_i}{\partial x_{kj}} \tag{12}$$

Integrating Equs. (6) and (7) into Equs. (11) and (12) gives

$$\begin{aligned} \frac{\partial t_i}{\partial x_{kj}} &= \frac{\partial\left[(K_k - I_0K - K_kE_0 + I_0KE_0)\bar{a}^i\right]}{\partial x_{kj}} = \\ &\frac{\partial(K_k)}{\partial x_{kj}}(I - E_0)\bar{a}^i = \\ &\frac{\partial\left[k_h(x_k,x_1),k_h(x_k,x_2),\cdots,k_h(x_k,x_n)\right]}{\partial x_{kj}}(I - E_0)\bar{a}^i = \\ &\left[\frac{\partial k_h(x_k,x_1)}{\partial x_{kj}},\frac{\partial k_h(x_k,x_2)}{\partial x_{kj}},\cdots\frac{\partial k_h(x_k,x_n)}{\partial x_{kj}}\right](I - E_0)\bar{a}^i \end{aligned} \tag{13}$$

Equ. (13) involves the partial derivative of the kernel function. We take the Gaussian kernel function as an example; we can obtain the derivation of the kernel function by combining literature [17]

$$k_h(x_k,x_i) = k_h(Vx_k,Vx_i) = e^{(-\frac{\|Vx_k - Vx_i\|^2}{\rho})} \tag{14}$$

where $V=[v_1,v_2,\cdots,v_m]^{\mathrm{T}}$, and $v_j = 1(j=1,2,\cdots,m)$.

The partial derivative of kernel function of variables v_j can be obtained from

$$\begin{aligned} &\frac{\partial k_h(x_k,x_i)}{\partial v_j} = \frac{\partial k_h(V\cdot x_k,V\cdot x_i)}{\partial v_j} = \\ &-\frac{1}{\rho}(v_jx_{kj} - v_jx_{ij})^2k_h(x_k,x_i)\Big|_{v_j=1} = -\frac{1}{\rho}(x_{kj} - x_{ij})^2k_h(x_k,x_i) \end{aligned} \tag{15}$$

where x_{ij} denotes the *j*th component in the *i*th component. The function of the inner product of two kernel partial derivative calculation is as follows:

$$\begin{aligned} &\frac{\partial k_h(x_k,x_i)k_h(x_k,x_l)}{\partial v_j} = \\ &-\frac{1}{\rho}\left\{(x_{kj} - x_{ij})^2 + (x_{kj} - x_{lj})^2\right\}k_h(x_k,x_i)k_h(x_k,x_l) \end{aligned} \tag{16}$$

Considering that different KPCs provide different reflections of deviation from the reference kernel feature space, real-time and dynamic weighting matrix *W* can be defined for each kernel principal component score of the currently monitored status based on Equs. (11), (12), (13), and (16). In this research, the normalization processing is performed to derive the weight of a coefficient

$$\begin{cases} \bar{C}_{T^2}(x_{kj}) = \dfrac{\left|C_{T^2}(x_{kj})\right|}{\sum_{j=1}^{m}\left|C_{T^2}(x_{kj})\right|} \\ \bar{C}_Q(x_{kj}) = \dfrac{\left|C_Q(x_{kj})\right|}{\sum_{j=1}^{m}\left|C_Q(x_{kj})\right|} \end{cases} \tag{17}$$

where weighting matrix W=diag(w_1,w_2, …,w_r) is a diagonal matrix. Given weighting matrix *W*, the weighted principal component t_W is

$$t_W = Wt_l. \tag{18}$$

Weighted statistics T_W^2 and Q_W are as follows:

$$\begin{cases} T_W^2 = [t_1,\ldots,t_r]W^T\Lambda^{-1}W[t_1,\ldots,t_r]^T \\ Q_W = \sum_{i=1}^{p}(\xi_it_i)^2 - \sum_{i=1}^{r}(\omega_it_i)^2 \end{cases} \tag{19}$$

where

$$\xi_i = \bar{C}_Q(x_{ki}), \quad i=1,\ldots,p \tag{20}$$

$$w_i(k) = \begin{cases} \bar{C}_{T^2}(x_{ki}), & i=2,\ldots,r \\ 1-\sum_{i=2}^{P}\bar{C}_{T^2}(x_{ki}), & i=1 \end{cases} \tag{21}$$

$$\omega_i(k) = \begin{cases} \bar{C}_Q(x_{ki}), & i=2,\ldots,r \\ 1-\sum_{i=2}^{P}\bar{C}_Q(x_{ki}), & i=1 \end{cases}. \tag{22}$$

Given that both the weighting matrix and the Λ matrix are diagonal matrices, we obtain the following:

$$T_W^2 = \left[t_1,\ldots,t_p\right] W^2 \Lambda^{-1} \left[t_1,\ldots,t_p\right]^{\mathrm{T}} \quad (23)$$

where W^2=diag(w_1^2,w_2^2, …,w_r^2) remains a diagonal matrix.

The Gaussian kernel is the most widely used function. In this study, the Gaussian kernel is employed, and the kernel estimator that becomes the Gaussian kernel is adopted in this research because of its good robustness to parameter change and its high degree of freedom [18]. The specific form of kernel function is as follows:

$$k_h(x,y) = e^{(-\frac{\|x-y\|^2}{\sigma})} \quad (24)$$

The kernel used in the structured KPCA is Gaussian kernel with width σ=5n based on the summary of the result of the IGBT fault detection.

B. Improved KPCA Optimization Process

As the circuit is symmetric in configuration, phase a in Fig. 1 is given as an example; phase a consists of four IGBTs, namely, S_{a1}, S_{a2}, S_{A1}, and S_{A4}. Therefore, four single-switch open-fault modes exist, the probability of two more IGBTs failure is quite low, and the multiple open switch faults modes consider only two switch failure modes, such as S_{a1} and S_{A4} faults.

In the proposed KPCA strategy, the weighting matrix emphasizes some special KPCs that capture dominant variations of current samples relative to the normal status. Complete monitoring procedures consist of the following steps:

In the normal steady-state condition of the inverter, 200 samples are obtained as training data. The normal data of the circuit are recorded as X, which contain 16 observed variables; these variables include three-phase current and voltage of upper half-bridge and lower half-bridge, neutral point voltage and current, and DC current and voltage.

Step 1. The kind of kernel functions is determined, normal operating data $X_{n\times m}$ are collected as modeling data, and the data of each variable are normalized into mean 0 and variance.

Step 2. The probability of each KPC is calculated, and the real-time and dynamic weighting matrix *W (k)* is determined based on the sensitivity analysis.

Step 3. The kernel matrix $K \in R^{n\times n}$ is computed, and the monitoring statistics (T^2 and *SPE*) of the normal operating data is calculated, and the confidence limit is determined.

Step 4. To process data from online collection, T^2 and the SPE are calculated by using the principal component model. If $T^2(k)$ statistic exceeds the confidence limit, then the detection of certain fault types is indicated. Then, the root cause is analyzed by using other fault diagnosis tools. Otherwise, Step 1 is repeated, and monitoring is continued.

IV. Experimental Results

In this section, the proposed KPCA monitoring method is applied in the IGBT open fault detection in the proposed topology (Fig. 1). The normal training data have 200 observations. Three kinds of IGBT faults are introduced here: the single IGBT fault, two IGBT faults of different bridge arm, and a hidden fault of the IGBT. The fault occurs in the 101st sample.

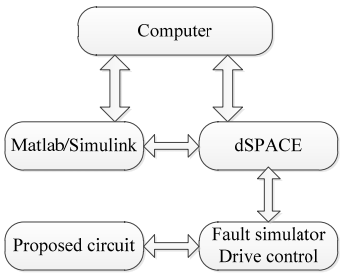

Fig. 3. Diagram of the hardware platform.

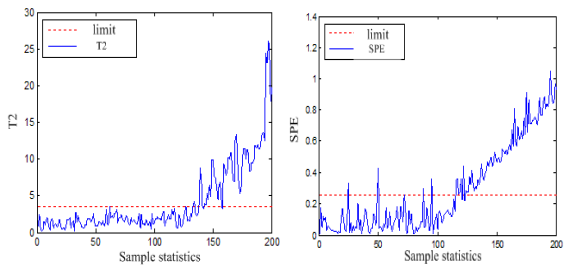

(a) Statistic plots with traditional KPCA method.

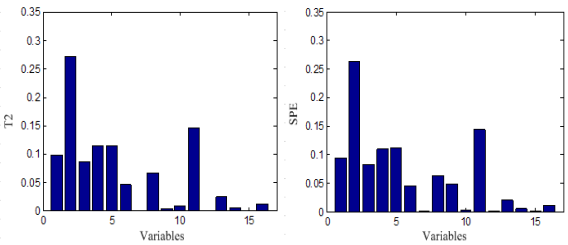

(b) Contribution plots for T^2 and *SPE* statistic.

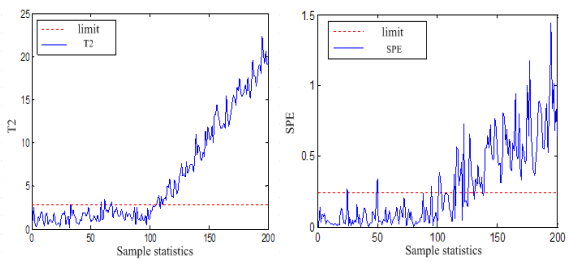

(c) Statistic plots with improved KPCA method.

Fig. 4. Detection of the IGBT open fault result of S_{a4}.

An experimental setup was developed using a DSP model TMS320C6713 to generate the command pulses for the proposed inverter. The IGBT type used for the experimental circuit is FUJI 1MBH60/D-100. In this research, an experiment on the power switches' open faults was conducted by disconnecting the summary bridge.

The operating conditions are given as follows: V_{dc}=230 V; L_{a1}= L_{a2}=…L_{C2}=2 mH; C_a=C_b=C_c=C_A=C_B=C_C=40 μF; $C = 8800\mu F$; R_a= R_b = R_c = R_A = R_B = R_C=25 mΩ; and

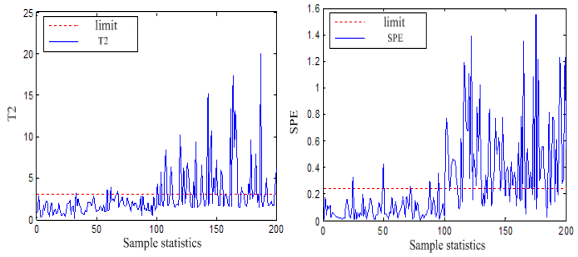

(a) Statistic plots with the traditional KPCA method.

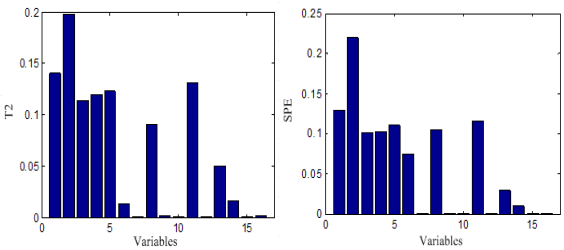

(b) Contribution plots for T^2 and SPE statistic.

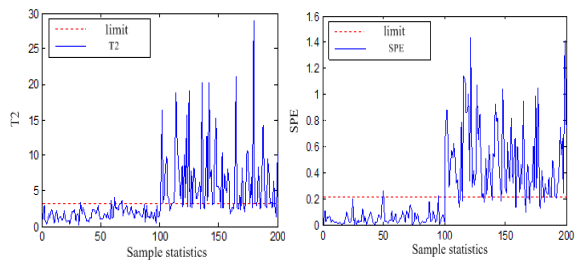

(c) Statistic plots with the improved KPCA method.

Fig. 5. Results of the detection of the IGBT open faults of S_{a1} and S_{a4}.

sampling period $T_s = 10$ μS. Rated frequency f is 400 Hz. The fourth leg alternately commutates its state at every sampling cycle. The detection of IGBT S_{a4} open fault results obtained by KPCA and improved KPCA are presented in Fig. 4

The detection of IGBT S_{a1} and S_{a4} fault results using KPCA and improved KPCA is presented in Fig. 4.

As shown in Figs. 4 and 5, T^2 and SPE statistic detection results of S_{a4} open faults are unsatisfactory at the beginning of the fault, and serious delay in detection took place after the fault occurred based on the traditional KPCA method. The detection results were improved by introducing the weighting strategies; this improvement indicates that the number of missed detection points is reduced significantly. The improved KPCA varies markedly when the fault occurs, thereby indicating that most deviations in information are highlight by the weighting matrix. Therefore, the information reflected on the KPCs, which should be highlighted, depends on different situations.

At the same time, the hidden fault of the new circuit fault is analyzed before the IGBT faults occurred. This method will present a high impedance state, and its mathematical model is equivalent to resistance and IGBT with two parts; the resistance is equal to the hidden fault value of the IGBT, assuming that the IGBT works in the ideal state [16]. An example is the hidden fault in S_{A1}, as shown in the fault

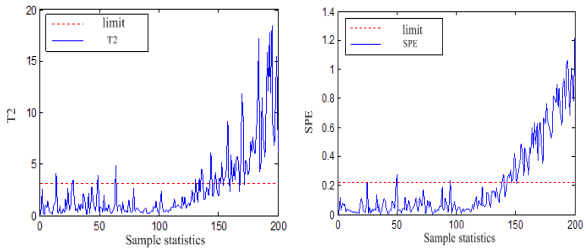

(a) Statistic plots with the traditional KPCA method.

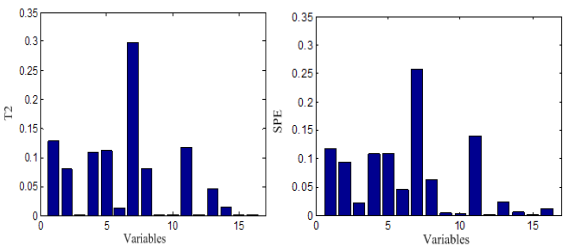

(b) Contribution plots for T^2 and SPE statistic.

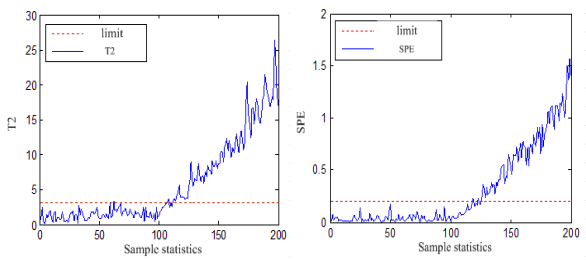

(c) Statistic plots with the improved KPCA method.

Fig. 6. Results of the detection of the IGBT hidden faults of S_{A1}.

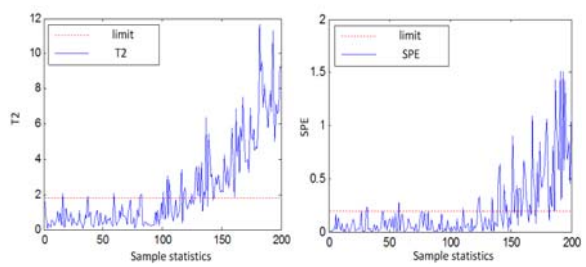

(a) Statistic plots with the improved KPCA method under R=80 Ω.

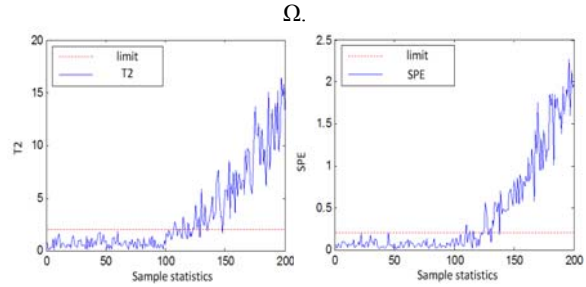

(b) Statistic plots with the improved KPCA method under R=40 Ω.

Fig. 7. Results of the detection of the IGBT open faults of S_{a1} and S_{A6}.

detection result in Fig. 6.

According to the result, using the KPCA method for fault detection, before the fault point of detection, gives a small amount of sample point that exceeds the control limit of statistics. This phenomenon is mainly due to the data

TABLE III
RESULTS OF THE CLASSIFICATION ACCURACY BY THE SVM

Fault modes	SVM with the traditional KPCA method	SVM with the improved KPCA method
S_{a1}	90%	95%
S_{a4}	95%	98%
S_{A1}	89%	93%
S_{A4}	95%	95%
S_{a1} andS_{A6}	71%	85%
S_{a1} and S_{a4}	77%	85%

containing substantial noise signal that has few outliers, thereby causing the normal sampling data to exceed the control limits.

To test the robustness of the improved strategy, results of the different load conditions were presented. The S_{a1} and S_{A6} open fault results detected by using improved KPCA under the condition of R=80 Ω and R=40 Ω are presented in Fig. 7. As shown in the results, the strategy has strong robustness to different load levels.

The KPCA strategy is used to extract the fault feature of the fault data to ensure that the fault modes of the inverter depend on the classification algorithm. This study adopts support vector machine (SVM) to classify the fault modes. The classification results (from 20 instances of experimental data) are shown in Table III. The classification accuracy results indicate that the improved KPCA method can highlight fault features and ensure easy classification of different fault modes by using SVM. Thus, the effectiveness of the improved method has been proven.

V. CONCLUSION

In this work, KPCA was employed to detect faults of IGBTs in the proposed inverter. Different weighting values were given to corresponding KPCs to highlight the KPCs that represent the main deviation information between the normal status and the current status, thereby improving sensitivity to fault detection. Furthermore, the proposed method is compared with the KPCA method, and results show that the selection of the weighting matrix based on the presented method achieves superior fault detection for different kinds of IGBTs in the proposed topology.

REFERENCES

[1] M. Schweizer, T. Friedli, and J. W. Kolar, "Comparative evaluation of advanced three-phase three-level inverter/converter topologies against two-level systems," *IEEE Trans. Ind. Electron*., Vol. 60, No. 12, pp. 5515-5527, Dec. 2013.

[2] J.-H. Zhou, B. Jia, X.-W. Zhang, and Y.-A. Chen, "A hybrid three-level neutral-point balance control strategy," *Proceeding of the CSEE*., Vol. 33, No. 24, pp. 82-89, Aug. 2013.

[3] S.-Y. Yang, D.-W. Xiang, A. Bryant, and P. Mawby, "Condition monitoring for device reliability in power electronic converters: A Review," *IEEE Trans. Power Electron.*, Vol. 25, No, 11, pp. 2734-2752, Nov. 2010.

[4] A. E. Ginart, D. W. Brown, P. W. Kalgren, and M. J. Roemer, "Online ringing characterization as a diagnostic technique for IGBTs in power drives," *IEEE Trans. Instrum. Meas.*, Vol. 58, No. 7, pp. 2290-2299, Jul. 2009.

[5] B. Wang, A. Hu, Y. Tang, and M Chen, "Analysis of voltage breakdown characteristic of IGBT," *Transactions of China Electrotechnical Society*, Vol. 26, No. 8, pp. 145-150, Aug. 2011.

[6] Y. Yu, S.-C. Jiang, R.-F. Yang, G. Wang, and D. Xu, "IGBT open circuit fault diagnosis method for inverter," *Proceedings of the CSEE*., Vol. 31, No. 9, pp. 25-30, Sep. 2011.

[7] B. Lu and S. K. Sharma, "A literature review of IGBT fault diagnostic and protection methods for power inverters," *IEEE Trans. Ind. Appl*., Vol. 45, No. 5, pp. 1770-1777, Sep./Oct. 2009.

[8] R. Szczesny, H. Piquet, and P. Kurzynski, "Fault detection and diagnosis in the electric drives," *European Conference on Power Electronics and Applications*, Vol. 2, pp. 995-1000, 1997.

[9] F. Zidani, D. Diallo, M. E. H. Benbouzid, and R. Na¨ıt-Sa¨ıd, "A fuzzy based approach for the diagnosis of fault modes in a voltage-fed PWM inverter induction motor drive," IEEE Trans. Ind. Electron., Vol. 55, No. 2, pp. 586-593, Feb. 2008.

[10] S. Khomfoi and L. M. Tolbert, "Fault diagnostic system for a multilevel inverter using a neural network," *IEEE Trans. Power Electron*., Vol. 22, No, 3, pp. 1062-1069, May 2007.

[11] C. Wang, L.-M. Jia, and X.-F. Li, "Fault diagnosis method for the train axle box bearing based on KPCA and GA-SVM," *Applied Mechanics and Materials*, Vol. 441, pp. 376-379, 2014.

[12] X.-G. Deng and X. M. Tian, "Fault diagnosis method based on immune kernel Principal component analysis," *Journal of Tsinghua University*, Vol. 48, No, 8, pp. 1794-1798, Oct. 2008.

[13] Q.-C. Jiang and X.-F. Yan, "Weight kernel principal component analysis based on probability density estimation and moving window and its application in nonlinear chemical process monitoring," *Chemometrics and Intelligent Laboratory Systems*, Vol. 127, pp. 121-131, Aug. 2013.

[14] J.-H. Hu, S.-S. Xie, W. Chen, S. Hou, and K.-L. Cai, "An aeroengine fault detection method based on kernel principal component analysis," *Journal of Propulsion Tecnology*, Vol. 29, No, 1, pp. 79-83, Feb. 2008.

[15] Q. Jiang and X. Yan, "Chemical processes monitoring based on weighted principal component analysis and its application," *Chemometrics and Intelligent Laboratory Systems*, Vol. 119, No, 7, pp. 11-20, Oct. 2012.

[16] J.-H. Hu, S.-S. Xie, G.-Q. Luo, F. Yang, and J.-B. Peng, "Fault identification method of kernel principal component analysis based on contribution plots and its application," *Systems Engineering and Electronics*, Vol. 30, No, 3, pp. 572-576, Mar. 2008.

[17] A. Rakotomamonjy, "Variable selection using SVM-based criteria," *Journal of Machine Learning Research*, Vol. 3, pp. 1357-1370, Mar. 2003.

[18] M.-Y. Zhao, C. Fu, L. Ji, K. Tang, and M.-T. Zhou, "Feature selection and parameter optimization for support vector machines: A new approach based on genetic algorithm with feature chromosomes," *Expert Systems with Applications*, Vol. 38, No. 5, pp. 5197-5204, May 2011.

Mao Lin was born in Shaanxi Province, China, in 1988. In 2010 and 2013, he received his B.S. and M.S. degrees in Electrical Engineering from the Air Force Engineering University, Xi'an, China, where he is currently working toward his Ph.D. degree, with focus on fault diagnosis for power electronics systems. His current research interests include power electronics, GPC control, and fault diagnosis of inverters.

Ying-Hui Li was born in Guangxi, China, in 1966. She received her B.S., M.S., and Ph.D. degrees in Electrical Engineering from Xi'an Jiaotong University, Xi'an, China, in 1987, 1990, and 2000, respectively. Since 1990, she has been a professor at the School of Aeronautics and Astronautics Engineering, Air Force Engineering University, Xi'an, China. Her research interests include nonlinear control theory on electronics systems, circuits, and control of high-efficiency integrated electric energy conversion in various industrial fields.

Liang Qu was born in Shaanxi Province, China, in 1987. He received his B.S. and M.S. degrees in Electrical Engineering from the Air Force Engineering University, Xi'an, China, in 2010 and 2013, respectively. He is currently working toward his Ph.D. degree at the Air Force Engineering University. His research interests include nonlinear control theory and flight safety.

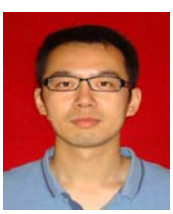

Chen Wu was born in Shaanxi Province, China, in 1990. He received his B.S. and M.S. degrees in Electrical Engineering from the Air Force Engineering University, Xi'an, China, in 2011 and 2014, respectively. He is currently working toward his Ph.D. at the Air Force Engineering University, where he is engaged in power electronic modeling. His current research interests include PFC circuit modeling and control research of the PFC circuit.

Guo-Qiang Yuan was born in Anhui Province, China, in 1991. He received his B.S. and M.S. degrees in Electrical Engineering from the Air Force Engineering University, Xi'an, China, in 2012 and 2015, respectively. He is currently working toward his Ph.D. degree at the Air Force Engineering University, where he is engaged in fault diagnosis for power electronics systems. His current research interest is fault diagnosis of inverters.